

A Photonic Tautochrone

W. Verstraelen^{*1,2}, S. Zanotti^{*1}, N. W. E. Seet^{1,2}, J. Zhao¹, D. Sanvitto^{1,3}, J. Zuñiga-Perez^{1,2}, K. Dini^{†1}, Y. G. Rubo^{†1,4}, and T. C. H. Liew^{†1,2,5}

¹Division of Physics and Applied Physics, School of Physical and Mathematical Sciences, Nanyang Technological University 637371, Singapore

²Majulab International Joint Research Unit UMI 3654, CNRS, Université Côte d’Azûr, Sorbonne Université, National University of Singapore, Nanyang Technological University, Singapore

³CNR NANOTEC Institute of Nanotechnology, Via Monteroni, Lecce 73100, Italy

⁴Instituto de Energías Renovables, Universidad Nacional Autónoma de México, Temixco, Morelos, Mexico

⁵Centre for Quantum Technologies, Nanyang Technological University Singapore

† Email: timothyliw@ntu.edu.sg, kevin.dini74@gmail.com, ygr@ier.unam.mx

Abstract

We propose to implement an optical analogue of the tautochrone property of the cycloid to allow the focusing of ultrashort pulses inside photonic systems. This allows to enhance nonlinear effects, resulting in orders of magnitude increase of nonlinearity-induced phase shifts, while employing low irradiances. Building upon the optical-mechanical analogy, we show how to produce optical limiters for temporal light pulses, and how to implement temporal bistability and even multistability with large numbers of states. Finally, we move this concept to the quantum realm and predict a tautochrone quantum blockade regime with a stronger antibunching.

Introduction.— In classical mechanics, there exists a trajectory for which particles starting simultaneously to slide down under constant acceleration and with no friction can arrive at the end of the curve at exactly the same time even if they had started at different positions along the curve. This remarkable effect is known as the tautochrone property of the cycloid and has been exploited in the design of accurate pendulum clocks [1]. Here, we ask whether it is possible to implement an analogous tautochrone effect in a photonic system and what this implies in the presence of nonlinearity.

We must first address a slight difference between mechanics and optics: in mechanics, particles follow a cycloid curve in a uniform gravitational field, while in optics photons move in straight lines. Nevertheless, we can easily imagine media in which photons move in a spatially non-uniform potential, which can be constructed thanks to a spatially-varying refractive index or to an adapted geometry of the photonic medium in which they are propagating. The key to the existence of a tautochrone effect is a spatially-varying potential energy, not necessarily a curved path.

The nonlinear Schrödinger equation provides a description of light propagating in nonlinear media. For photonic particles with a parabolic dispersion and parabolic potential in the direction transverse to propagation, it can be written as:

$$i\frac{\partial\psi(\mathbf{x},t)}{\partial t} = \frac{1}{2}(-\nabla^2 + \mathbf{x}^2 - i\gamma + 2|\psi(\mathbf{x},t)|^2)\psi(\mathbf{x},t) + F(\mathbf{x},t). \quad (1)$$

*These authors contributed equally.

This equation describes, for example, the behaviour of light in planar Fabry-Perot microcavities, where light is confined in the microcavity growth direction but spreads in the plane $\mathbf{x} = (x, y) = (r \cos \phi, r \sin \phi)$. In such a case, dissipation is accounted for with rate γ , the nonlinear term represents a Kerr-type nonlinearity, and F represents the amplitude of a coherent driving field (e.g., a laser source). We use dimensionless units (see the Appendix for transformation to real variables).

If the system is driven with an ultrashort laser pulse that is also spatially wide, light is injected at different positions in space at the same moment of time. If the pulse is only slowly varying in the transverse coordinate, which is commonly the case for a laser pulse aligned with the propagation direction (or growth direction for microcavities), we can note that the initial energy of the light is dominated by its potential energy, while its kinetic energy is initially vanishing. This is analogous to the initial conditions of classical particles initialized on a cycloid curve with zero velocity.

Given that the oscillation frequency of particles in a parabolic potential is independent of their energy, every particle is now accelerated toward the center of the parabolic potential and will reach $\mathbf{x} = 0$ at the same time (see Fig. 1a). In the linear regime without dissipation, an initial Gaussian wavepacket evolves as $|\psi(t, \mathbf{x})|^2 \propto \exp\{-\mathbf{x}^2/(2|\sigma(t)|^2)\}$ (see, e.g., Ref. [2] and Supplemental Material for full solution), where the time evolution of the width is:

$$|\sigma(t)|^2 = \sigma_0^2 \cos^2 t + \frac{1}{4\sigma_0^2} \sin^2 t, \quad (2)$$

and $\sigma_0 = \sigma(0)$ defines the initial width. We note that for a large enough initial width, the wavepacket collapses to a point. This behaviour is shown in Fig. 1b. While in theory larger and larger initial widths give arbitrarily tighter focusing, we should note that the paraxial approximation will eventually break down in this simple picture. In any case, a strong focusing effect is clearly achieved.

We propose that the aforementioned focusing effect can have strong implications in nonlinear photonics by enhancing the effect of interactions in nonlinear media. We show theoretically that it allows orders of magnitude enhancement of nonlinear phase shifts, temporal bistability, temporal multistability, and quantum blockade. Most importantly from the experimental point of view, we also present explicit designs of photonic structures for the realization of the required photonic potential.

Interaction-induced phase-shift.— While the simplest way to detect interactions in a nonlinear photonic system is to look for an energy shift of the photonic modes involved, the most accurate measurements, which have sensitivity down to the few photon level [4], rely on phase shifts. In Fig. 1c, we find that the phase shift measured in the center of a two-dimensional parabolic potential jumps by π in the linear regime every time the particles undergo a focusing event. The phase shift is enhanced in the nonlinear regime and we define the nonlinear-induced phase shift as the difference of the phase in the nonlinear and linear regimes in Fig. 1d. Remarkably, the nonlinear-induced phase shift is over two orders of magnitude larger in the parabolic trap as compared to the same pulse without the parabolic potential and the same nonlinear interaction strength.

Optical Limiter.— Aside the prospect of enhanced nonlinear-induced phase shifts, we can also ask if related nonlinear intensity effects would also be enhanced. Among the most fundamental of Kerr nonlinear effects is the optical limiter effect, whereby the injected intensity from a resonant continuous wave laser increases sublinearly with the laser power and which is used to protect devices from overload (including lasers themselves). This effect relies on interactions shifting the photonic field out of resonance with the pumping laser. To achieve this in the tautochrone case we should ensure that all light is injected at the same time, which would necessitate using short pulses and, thus, restricting to broadband photonic fields and driving fields. Instead, we propose to consider a periodic driving of the system with a sequence of ultrashort pulses whose period matches twice the focusing time.

In the absence of interactions, we obtain the result shown in Fig. 2a. Here we have also ensured that subsequent pulses have a phase shift of π and are spatially inverted such that each pulse adds constructively to the field and respects $F(\mathbf{x}, t = (2n + 1)\pi) = -F(-\mathbf{x}, t = 2n\pi)$. We account now also for dissipation, considering the regime where the dissipation (lifetime) is comparable to the repetition period. In Fig. 2b, we find that in the nonlinear regime the intensity is significantly reduced. This is because the nonlinear phase shifts desynchronize the signal from the driving pulses.

Figure 3(a) shows that the increase of the photonic field intensity with laser power in the aforementioned pulsed excitation case follows an optical limiter-like curve. This curve appears more nonlinear for the same range of (time-averaged) field intensity when compared to the traditional optical limiter achieved under continuous wave excitation, as represented by the almost linear dependence shown in Figure 3(a) (for a fair

comparison between the pulsed and CW regimes, we consider the same parabolic potential and dissipation rate).

Bistability.—Aside the optical limiter effect, a Kerr nonlinear resonator can also demonstrate bistability under continuous wave excitation [5] when the driving field is tuned slightly out of resonance. To make use of the tautochrone mechanism, we consider an extension of the phase delay between subsequent pulses exploited in the optical limiter effect as an analogue of the detuning in the continuous wave bistable regime. Notably, the excitation pulses remain on resonance, in contrast to conventional bistability schemes based on frequency detuning. Figure 3b shows that an extra 0.25π dephasing of the pumps compared to the optical limiter results in bistability and hysteresis in the system. The physical interpretation is that when there is a low intensity in the system, the focusing and defocusing sequence in the tautochrone is not synchronized with the phases of the repeating driving pulses. However, with some intensity in the system, interactions allow synchronization and maintenance of a high intensity. While traditionally bistability is used to describe a system with two stationary states of the system, we use the term here to describe two spatially and temporally oscillating states that are nevertheless stable and exist under the same conditions.

Multistability.—The aforementioned effect may seem like an over-complicated analogue of already well-established bistability. However, what is quite different to the usual bistability under continuous wave excitation is that the tautochrone mechanism allows generalization to support multiple stable states, with obvious potential applications in communication and information processing. We recall that the sequence of pulses excites an oscillating state that focuses and defocuses periodically. In addition to this state and its associated pulse sequence, we could apply another set of pulses at intermediate times. To minimise cross-interactions between the two pulse sequences, the pulse profile is chosen as a Gaussian multiplied by the square of the radial coordinate, so that the excitation vanishes at the centre. This would effectively enable to double the pulse repetition rate and allow for two states of light oscillating simultaneously in the system, with each state focusing with the arrival of alternate pulses. Figure 4 shows that four different spatially and temporally oscillating states are now supported under the same conditions.

Interestingly, the multistable regime can be easily generalized to generate a larger number of coexisting stable states. In the Appendix, instead of doubling the pulse repetition rate, we quadruple it and find that sixteen different stable states are supported under the same conditions.

Quantum Blockade.— So far, we have discussed a photonic tautochrone and its consequences in the nonlinear regime within the framework of semi-classical theory, including the optical limiter effect. This is appropriate for large numbers of particles where the mean-field approximation offers a good description of coherent states. Going beyond such an approximation, a quantum treatment of the conventional optical limiter (i.e., under continuous drive) gives rise to the photon [10] or polariton [11] blockade effect. While the classical optical limiter uses an optical density to shift out of resonance the optical field and the coherent driving field, the quantum blockade allows multiparticle quantum states to shift out of resonance and be effectively suppressed. The result is a non-classical antibunched state, characterized by a second order correlation function $g^{(2)}$ dropping below 1 (for a multiparticle state) and approaching 0 for a perfect single particle state. For this effect to take place, one requires the interaction strength between two particles to exceed the linewidth of the system.

While exciton-polaritons are known for their nonlinearity, which is stronger than in conventional nonlinear photonics, only the onset of the polariton blockade, with second order correlations below but still close to 1, have been attained experimentally [12, 13]. We note that such single photon states are, beyond fundamental interest, important building blocks for many applications, including quantum technologies such as quantum key distribution and boson sampling, as well as to biological research [15, 16].

We now consider a fully quantum theory of our photonic tautochrone, introducing the density matrix ρ to represent the quantum state of the system, which evolves according to the master equation:

$$i\hbar \frac{\partial \rho}{\partial t} = [\hat{\mathcal{H}}, \rho] + i\tilde{\gamma} \hat{\mathcal{L}}(\rho) \quad (3)$$

Here $\hat{\mathcal{H}}$ is the Hamiltonian, which accounts for parabolic kinetic and potential energies together with nonlinear interactions and is defined in the Appendix. The Lindblad superoperator $\hat{\mathcal{L}}$ describes the dissipation of particles at rate $\tilde{\gamma}$. Whereas the conventional quantum blockade is typically calculated for a single quantum mode, we do need to account for spatial dependence explicitly to model the tautochrone behaviour. While this approach results in an intractable size of the density matrix, the master equation can be simulated (to

arbitrary accuracy) using a stochastic sampling of the phase space within the Positive P approach (see the Appendix for a full description). The full (equal time) second order correlation function of the trap created by the tautochrone effect is defined as:

$$g^{(2)}(t) = \frac{\iint \langle \hat{\psi}^\dagger(\mathbf{x}, t) \hat{\psi}^\dagger(\mathbf{x}', t) \hat{\psi}(\mathbf{x}', t) \hat{\psi}(\mathbf{x}, t) \rangle d^2\mathbf{x} d^2\mathbf{x}'}{\left(\int \langle \hat{\psi}^\dagger(\mathbf{x}, t) \hat{\psi}(\mathbf{x}, t) \rangle d^2\mathbf{x} \right)^2} \quad (4)$$

where $\hat{\psi}(\mathbf{x}, t)$ annihilates a particle at position \mathbf{x} and time t ; the angled brackets denote the expectation value. Figure 5 compares the value of $g^{(2)}$ under periodic pulsed excitation to that calculated under continuous wave excitation with the same spatial profile for the same parabolic potential. Although the mechanism of the optical limiter is somewhat different under periodic pulsed excitation, we find that it also results in antibunching in the quantum limit. More remarkably, the strength of the antibunching is twice as strong around $N \sim 1$. Modest system parameters were assumed, such that the conventional blockade under continuous wave excitation matches experimental reports [12, 13]. Thus, even using realistic physical parameters, the tautochrone effect displays a clear quantitative advantage and appears as an interesting approach to enhance not only nonlinear effects but also, thanks to them, nonlinear quantum effects. In the next section we describe how to build a photonic system displaying the effect introduced in this work.

Designs for Optical Potential Engineering.— In principle, any photonic system with a spatially varying refractive index or effective refractive index would be suitable for the engineering of a parabolic potential for photons. Exciton-polaritons in microcavities are a good candidate system given that, indeed, parabolic traps have already been realized experimentally some time ago using different techniques to modify the local exciton-potential [6, 7] or the local photonic-potential thanks to a spatially varying cavity thickness [8]. In general, exciton-polaritons are renowned for their effective Kerr nonlinearity and there are, thus, also other options for potential engineering as described in [9]. Overall, the current fabrication state-of-the-art ensures the technological feasibility of microcavities implementing the necessary photonic or polaritonic potentials. For completeness, we give a complete theoretical simulation of such a system using nonlinear Maxwell-Bloch finite-difference time simulations in the Appendix (this also shows that our results are not dependent on the paraxial approximation implicit in Eq. 1).

Discussion.— One may wonder whether the aforementioned behavior could also occur with a non-parabolic potential or non-parabolic kinetic energy term. In a classical single-band model, the Hamiltonian for a particle in any one-dimensional potential can be written as a function of position x and momentum p . Regardless of the Hamiltonian, it could also be written in terms of the canonical variables $I = (x^2 + p^2)/2$ and $\theta = \text{atan}(x/p)$. Here $\theta = \pi/2$ corresponds to initial conditions where particles can have different values of position x , but zero momentum p ; $\theta = \pi$ corresponds to the case where a particle has position $x = 0$. Hamilton's equation of motion is $\dot{\theta} = \partial H / \partial I$. The only way for all particles to arrive at $x = 0$ at the same time, regardless of their different initial positions (which give different values of I), is to choose $H \propto I$, such that $\dot{\theta}$ is independent of I . This implies a parabolic potential and parabolic kinetic energy. Mathematically, it appears that H could also be supplemented with some function of θ without breaking the tautochrone behavior; however, such a dependence seems exotic from a physical point of view. Note that in a 2D case, similarly strong nonlinear effects could also be promoted by focusing particles on a line (caustic), and a wider class of effective Hamiltonians could lead to such behaviour.

We have focused on the excitation of a photonic tautochrone by a coherent pulsed excitation. One could also ask what happens under a non-resonant gain. Under a simple Landau-Ginzburg type model [14], which is commonly used in the description of exciton-polariton lasers, we find that an effective optical limiter response can be realized above some threshold. This is quite different to the usual case of continuous wave excitation, where the Landau-Ginzburg model typically results in a linear growth of intensity above threshold. As the effects that we have discussed in this paper take the optical limiter effect as a foundation, we speculate that many of them would also be possible under non-resonant gain as well.

Finally, although we have considered a spatially uniform dissipation, systems with spatially varying dissipation could offer further advantages. A limitation of the conventional quantum blockade effect is that there is a large uncertainty in the time of generation of a single photon (which can be considered a consequence of the uncertainty principle and monochromatic frequency distribution). In principle, a system could be engineered so that dissipation is strongest at the center of the trap. This would allow a higher

probability of emission at the specific times when the polychromatic wavepacket has focused to the trap center.

Conclusion.— An optical pulse in a medium with an effective parabolic potential becomes focused due to an analogue tautochrone property where all particles reach the center of the potential at the same time. This spatiotemporal focusing results in the enhancement of nonlinear-induced phase shifts by orders of magnitude. Despite the broad frequency range, analogues of the optical limiter effect, bistability, and multistability with large numbers of states can be arranged under periodic pulsed excitation. The periodic focusing of wavepackets results in an increased sensitivity to interactions, which ultimately manifests in a stronger quantum blockade.

Acknowledgements.— SZ, KD, JZP, & TCHL acknowledge support from the National Research Foundation grant N-GAP (NRF2023-ITC004-001). JZ & TCHL acknowledge support from the Singapore Ministry of Education (MOE) Academic Research Fund Tier 3 grant “Quantum Geometric Advantage” (MOE-MOET32023-0003). WV, DS, & TCHL acknowledge support from the EU under grant “Quantum Optical Networks based on Exciton-polaritons” (Q-ONE). NWES, JZP, DS, & TCHL acknowledge support from the EU under EIC Pathfinder Open project “Polariton Neuromorphic Accelerator” (PolArt, Id:101130304). YGR & TCHL acknowledge support from DGAPA-UNAM, Grant PAPIIT No. IN108524.

References

- [1] R.A. Proctor, "A Treatise on the Cycloid and All Forms of Cycloidal Curves, and on the Use of Such Curves in Dealing with the Motions of Planets, Comets, &c., and of Matter Projected from the Sun", Longmans (1878).
- [2] D J Tannor, *Introduction to Quantum Mechanics: A Time-dependent Perspective* (Univ. Sci. Books, Sausalito, California, 2007).
- [3] I Carusotto & C Cuiuti, *Rev. Mod. Phys.*, **85**, 299 (2013).
- [4] T Kuriakose, P M Walker, T Downling, O Kyriienko, I A Shelykh, P St-Jean, N Carlon Zambon, A Lemaitre, I Sagnes, L Legratier, A Harouri, S Ravets, M S Skolnick, A Amo, J Bloch, & D N Krizhanovskii, *Nature Photon.*, **16**, 566 (2022).
- [5] A Baas, J P Karr, H Eleuch, & E Giacobino, *Phys. Rev. A*, **69**, 023809 (2004).
- [6] R Balili, V Hartwell, D Snoke, L Pfeiffer, & K West, *Science*, **316**, 1007 (2007).
- [7] G Tosi, G Christmann, N G Berloff, P Tsotsis, T Gao, Z Hatzoupoulos, P G Savvidis, & J J Baumberg, *Nature Phys.*, **8**, 190 (2012).
- [8] B Besga, C Vaneph, J Reichel, J Estève, A Reinhard, J Miguel-Sánchez, A Imamoğlu, & T Volz.
- [9] C Schneider, K Winkler, M D Fraser, M Kamp, Y Yamamoto, E A Ostrovskaya, & S Höfling, *Rep. Prog. Phys.*, **80**, 016503 (2017).
- [10] A Imamoğlu, R J Ram, S Pau, & Y Yamamoto, *Phys. Rev. A*, **53**, 4250 (1996).
- [11] A Verger, I Carusotto, & C Ciuti, *Phys. Rev. A*, **76**, 115324 (2007).
- [12] A Delteil, T Fink, A Schade, S Hofling, C Schneider, & A Imamoğlu, *Nature Mater.*, **18**, 219 (2019).
- [13] G Munoz-Matutano, A Wood, M Johnson, X Vidal Asensio, B Baragiola, A Reinhard, T Volz, A Lemaitre, J Bloch, A Amo, B Besga, & M Richard, *Nature Mater.*, **18**, 213 (2019).
- [14] J Keeling & N G Berloff *Phys. Rev. Lett.*, **100**, 250401 (2008).
- [15] C. Couteau, S. Barz, T. Durt, T. Gerrits, J. Huwer, R. Prevedel, J. Rarity, A. Shields, and G. Weihs, "Applications of single photons to quantum communication and computing," *Nat. Rev. Phys.* **5**, 326–338 (2023).

- [16] C. Couteau, S. Barz, T. Durt, T. Gerrits, J. Huwer, R. Prevedel, J. Rarity, A. Shields, and G. Weihs, “Applications of single photons in quantum metrology, biology and the foundations of quantum physics,” *Nat. Rev. Phys.* **5**, 354–363 (2023).

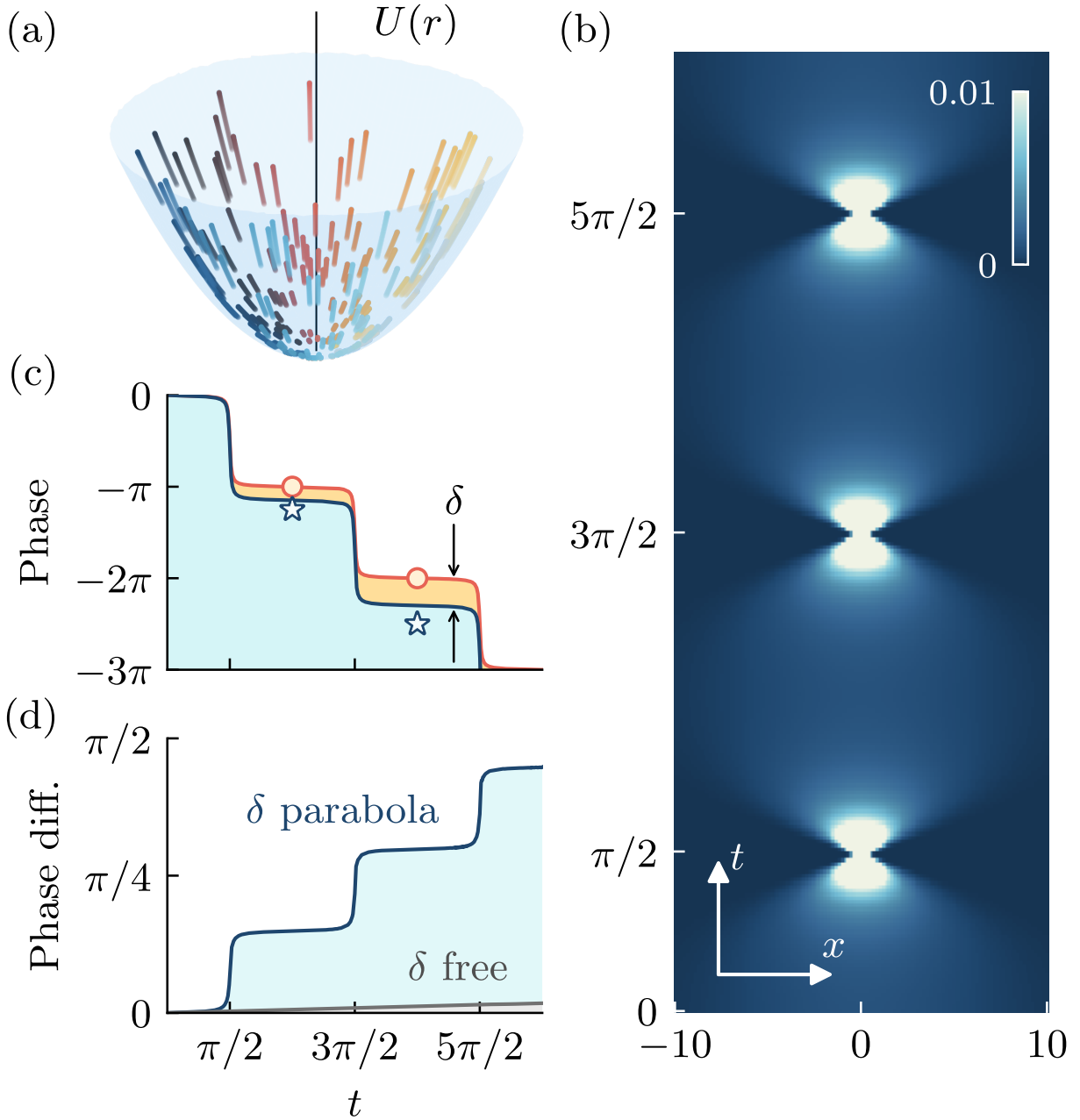


Figure 1: **Photonic Tautochrone.** a) A pulsed excitation initializes particles at different positions of a parabolic potential. The particles are then accelerated toward the center corresponding to a focusing of light. b) A space-time plot of intensity at $y = 0$ shows that the focusing occurs at $t = \pi/2$ and integer delays of π thereafter. The colour scale has been saturated at $1/100$ the peak value. c) The phase of light in the center undergoes a jump of π after each focusing event (red); the shift is enhanced in the nonlinear regime (blue). Circles and stars mark the times and phases of the excitation pulses for the optical limiter and bistable regimes, respectively. d) Nonlinearity-induced phase shift for free particles (grey) and in the presence of a parabolic potential (blue). The initial field $\psi(x)$ is normalized to unity. Other parameters: $\sigma_0 = 5$; $\gamma = 0$.

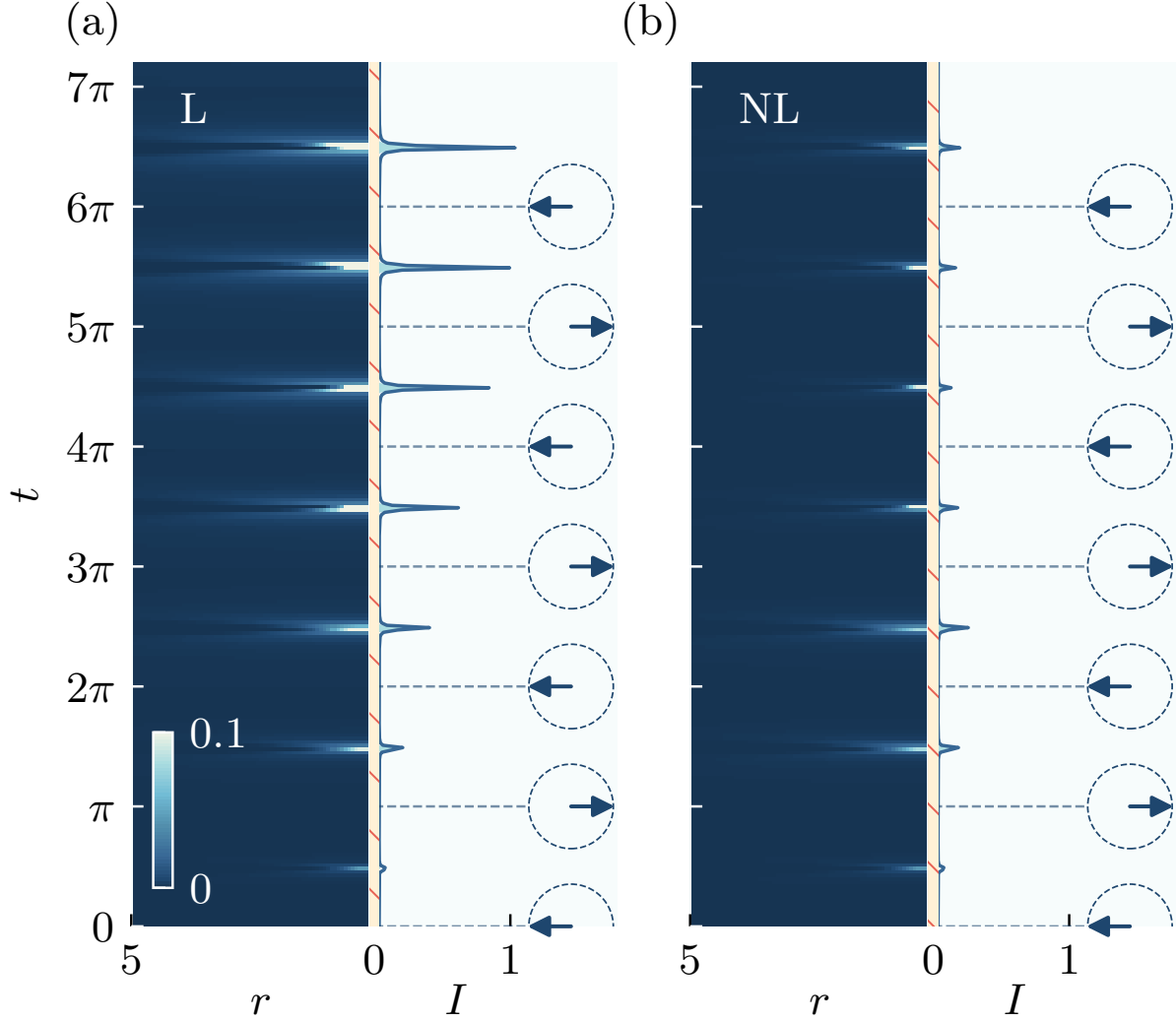


Figure 2: **Pulsed Excitation.** (a) Intensity $|\psi(r,t)|^2$ (left) and its linecut at $r = 0$ (right) under periodic excitation without interactions, computed from Eq. 1 ($\psi(r, \phi, t)$ is independent of ϕ , so we do not plot the ϕ dependence). The repetition period was π , $\gamma = 1/(2\pi)$, and all other parameters were the same as in Fig. 1, with the spatially integrated pulse intensity set to unity. Arrows mark the pulse arrival times, and their orientation encodes the excitation phase; these pulses correspond to the circles shown in Fig. 1(c). We have chosen the driving term to have a Gaussian form in space. (b) Same analysis as in (a), but with nonlinear interaction included, which leads to a pronounced quenching of the peaks intensity. Intensities in (a) and (b) have been normalised to the maximum peak intensity in (a). For subsequent pulses, the system eventually settles in a state where the intensity is periodic in time.

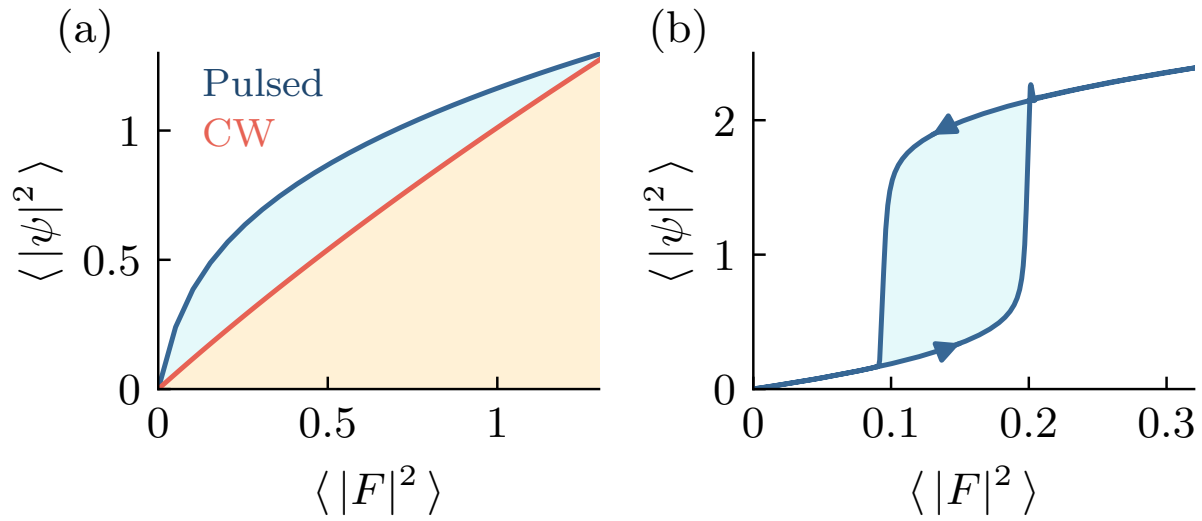


Figure 3: **Optical Limiter & Bistability.** a) Power dependence of a photonic tautochrone under periodic pulsed excitation, compared to the same setup under continuous wave (CW) excitation. $\langle |\psi|^2 \rangle$ and $\langle |F|^2 \rangle$ represent spatially integrated and time-averaged field and driving intensities, respectively. Parameters were the same as in Fig. 2b. As the overall response to the CW excitation is weaker than the pulsed case, $|F|^2$ is multiplied by a factor of 100 for CW excitation. b) Same as (a) but with the phase delay between subsequent pulses set to 1.25π . The driving field intensity is slowly ramped up and down, revealing a hysteresis region (shaded).

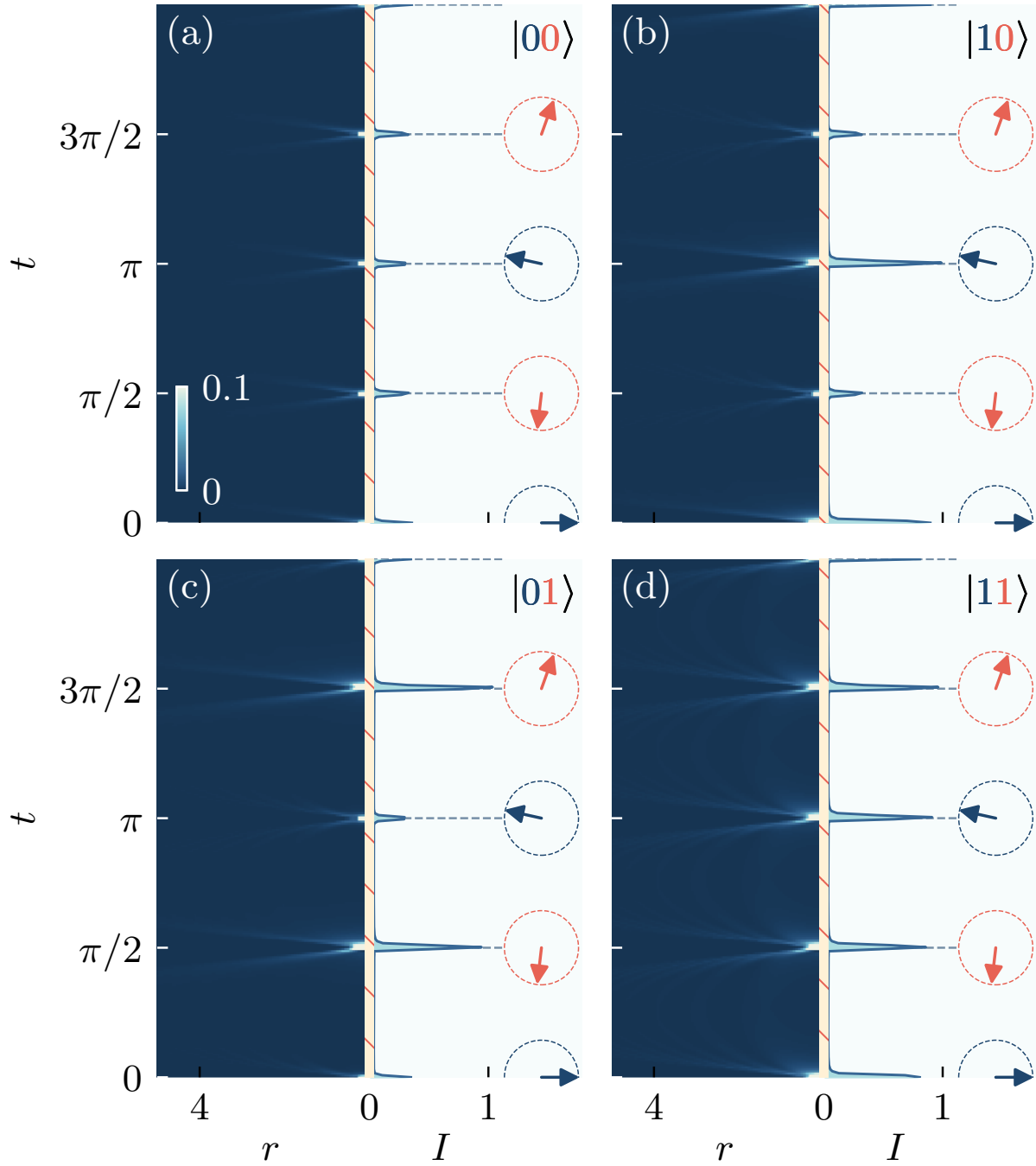


Figure 4: **Multistability.** A photonic tautochrone is driven by two pulse trains with a repetition period of $\pi/2$, each encoding a different bit. Under these conditions, a hysteresis curve analogous to that in Fig. 3b is obtained, and the pulse intensity is chosen to operate within the multistable regime. Depending on the excitation history, four distinct oscillating states can be produced. Panels (a–d) correspond to the four possible bit encodings $|00\rangle$, $|01\rangle$, $|10\rangle$, and $|11\rangle$, respectively. All remaining parameters are the same as in Fig. 3b. The colour scales have been saturated to $1/10$ of the peak intensity in (d). Unlike in Fig. 2, here we show the intensity after many pulses such that the initial transient dynamics has been completed.

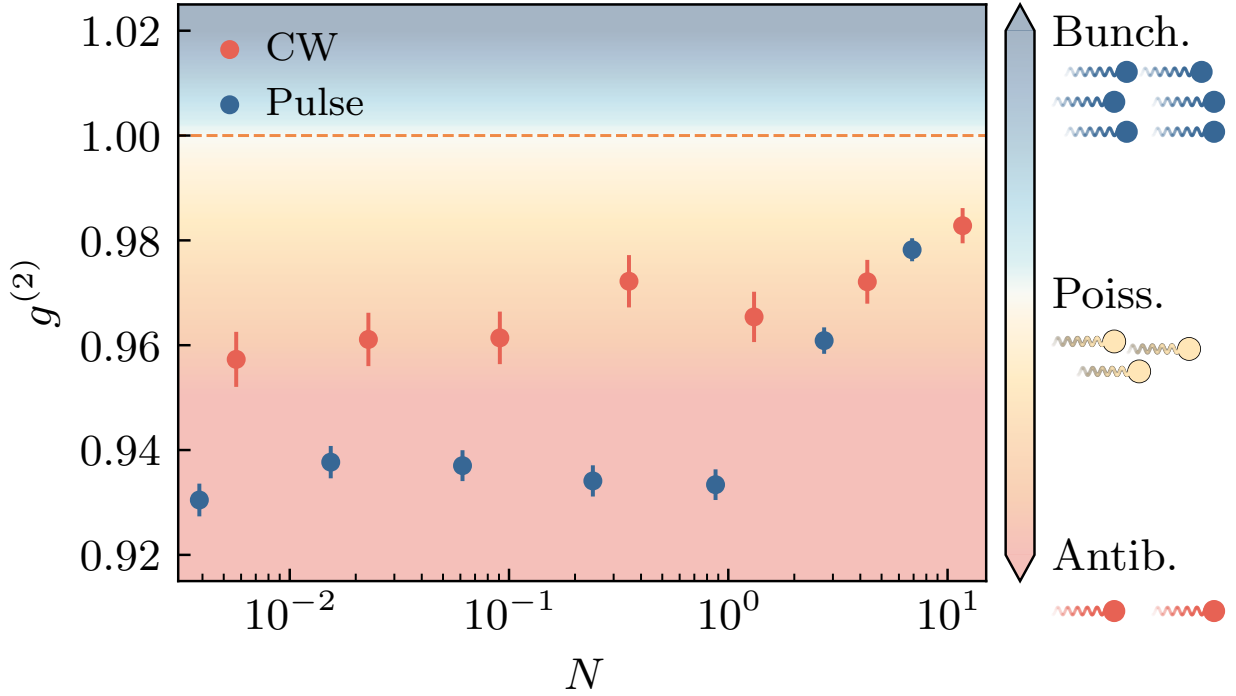


Figure 5: **Photon blockade.** For sufficient photon nonlinearity α , conventional photon blockade will shift the multi-photon states out of resonance causing antibunching, as is well known under continuous wave (CW) excitation, also in the parabolic trap. The enhancement of interactions through pulses in the tautochrone scheme however, is able to enhance such antibunching. Simulations were done over fixed $\alpha = 0.1 \omega l^2$, where l, ω are the harmonic oscillator length and frequency, respectively, while varying F_0 , which affects also the average particle number N . Refer to supplementary for details.